Quantitative MR-guided transient shear wave imaging for tissue elasticity assessment

Yu Liu, Jingfei Liu, Brett Z. Fite, Josquin Foiret,
J. Kent Leach, Katherine W. Ferrara
Department of Biomedical Engineering
University of California, Davis, CA 95616
Contact author: kwferrara@ucdavis.edu

***Abstract*—Elastography is an efficient alternative to the traditional palpation method of assessing tissue stiffness. Magnetic resonance imaging (MRI) provides a three-dimensional (3D) high-resolution view of the surrounding anatomy during interventions. Therefore, the development of MRI-based elastographic strategies is desirable for multiple clinical applications. In this work, we developed a new transient magnetic resonance elastography (t-MRE) protocol that improved visualization of transient shear wave propagation and applied this protocol to quantify tissue elasticity *in vitro* using tissue-mimicking phantoms. The MRE data were cross-validated with measurements acquired under ultrasound (US) guidance and mechanical testing (MT). Following a three-pulse excitation, the t-MRE protocol was applied to visualize planar shear waves propagating 2 to 30 mm away from the excitation location. Differences in shear modulus on the order of 1 kPa were reliably detected and estimates of shear elasticity by US-based elastography and MT differed by less than 7% of the MT gold standard value. Moreover, biologically-relevant inclusions were detected in tissue-mimicking phantoms and mapped in 3D by t-MRE.**

Keywords- Magnetic Resonance Imaging (MRI), Transient Shear Wave, Magnetic Resonance Elastography (MRE), Mechanical Test (MT)

I. INTRODUCTION

Elastography can provide a noninvasive assessment of the mechanical properties of intact tissue. The most prominent current elastographic techniques use US or MRI imaging to map changes in tissue in response to a perturbation and produce an anatomical image for comparison [1]. Elastography has been reported to differentiate cancerous tumors from surrounding tissue, distinguish between malignant and benign lesions, and track changes with therapy [2-5]. Recently, Bercoff et al proposed a Supersonic Shear Imaging (SSI) approach by combining Acoustic Radiation Force (ARF) excitation and ultrafast US imaging for transient elastography [6]. The technique creates quasi-planar shear waves by transmitting a pulse train and changing the US focal depth within the train. The combination of ARF and ultrafast US imaging produced an image of shear wave propagation in less than 0.01 ms and facilitated the creation of a quantitative elasticity image. This technique has been applied for breast cancer diagnosis [7].

MR elastography (MRE) was first introduced in 1995, and in this technique an external vibration was used to stimulate shear waves (SW). These shear motions were encoded into the MR phase images by adding motion encoding gradients (MEGs) within conventional MR pulse sequences [8, 9]. Based on the shear wave propagation speed, the stiffness of the tissue was reconstructed [10, 11]. One of the disadvantages of MRE is that an external mechanical vibrator is required to generate shear waves, and this can limit the penetration depth due to attenuation and reflection [12, 13]. Furthermore, the shear wave velocity estimation is challenging due to reflections and standing wave patterns.

Previously, we demonstrated that a protocol combining MR-acoustic radiation force imaging (MR-ARFI) with shear wave velocity estimation has potential applications in interventional radiology [14]. Focal displacement and shear wave velocity estimates were obtained with the same MR-ARFI acquisition and the displacement was used to detect changes in tissue properties with high intensity focused US (HIFU) treatment. Shear waves were visualized *in vitro* and the shear wave velocity was estimated by changing the delay between the motion encoding gradients and US pulses. However, shear wave propagation could not be detected near the excitation site due to the requirement for a long excitation with this protocol. In order to improve the visualization of transient shear wave propagation, here, we integrated supersonic US excitation and MR imaging to create a new elasticity protocol. Tissue elasticity was quantified under both MR and US guidance and shear modulus values were then validated with those obtained from MT.

II. METHODS

MRgFUS was performed using a Bruker Biospec 70/30 (7T) small animal scanner (Bruker BioSpin MRI, Ettlingen, Germany) with a 154 mm internal diameter circularly-polarized coil (Bruker), an MR-compatible pulser and 2D positioning system (Image Guided Therapy, France), and an MR-compatible 16-element annular array transducer (IMASONIC SAS, France). The US center frequency was 3 MHz and the array aperture was 48 mm in diameter. The radius of curvature of the array was 35 mm with a -6 dB focal volume of $0.5 \times 0.5 \times 2$ mm^3.

A. *Transient magnetic resonance elastography (t-MRE) protocol*

MR images were acquired using a modified two-dimensional (2D) spin-echo imaging sequence (Fig. 1). Three US pulses (3 MHz, 0.45 ms pulses with 4.5 mm spacing between transmit foci and 12.5 MPa peak negative pressure (PNP)) were sequentially excited creating a planar SW. The MRI acquisition parameters were as follows: repetition time (TR)/ echo time (TE)/ flip angle (FA) = 500 ms/26.1 ms/90°; refocusing angle: 180°; MEG = 140 mT/m; MEG duration = 1 ms; field of view (FOV) = 80 x 80 mm^2;

978-1-4673-9897-8/16/$31.00 ©2016 IEEE

matrix (MTX) = 240 x 240; slice thickness (ST) = 1 mm, 1 slice, number of excitations/averages (NEX) = 1; bandwidth (BW) = 27 kHz. A series of nine images was acquired with delay times, t_d, ranging from 0.45 ms to 4.05 ms.

The shear modulus μ was then estimated using the time-of-flight (TOF) method as following:

$$\mu(x,z) = \rho c^2(x,z) \quad (1)$$

in which the mass density of the medium material, ρ, is assumed as 1000 kg/m^3 and $c(x,z)$ is the local shear wave speed as a function of the x and z spatial coordinates.

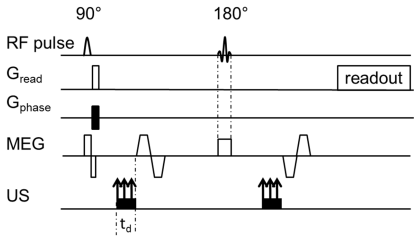

Fig. 1. t-MRE sequence

B. US guided shear wave imaging (USgSWI) setup

The USgSWI measurement was performed with a Vantage 256 (Verasonics, WA, USA) and a Phillips L7-4 transducer. To generate the SW, pulse parameters were 4.3 MHz center frequency, 10 MPa PNP and a 100 µs pulse length. Pulses were transmitted with 5 mm spacing between transmit foci. US images were obtained with a 5.2 MHz center frequency, using 20 acquisitions of 50 frames in flash imaging mode with a PRF of 10 kHz. Shear wave displacements were tracked using 1D normalized cross-correlation with a tracking window of 2.4 mm (8 wavelengths). The local inversion method (LIM) was used to estimate the shear modulus, where

$$\mu(x,z) \approx \frac{\rho}{\Delta\omega} \int \frac{\left| FT\left\{ \frac{\partial^2 d(x,z,t)}{\partial t^2} \right\} \right|}{\left| FT\left\{ \frac{\partial^2 d(x,z,t)}{\partial x^2} + \frac{\partial^2 d(x,z,t)}{\partial z^2} \right\} \right|} \quad (2)$$

in which $\Delta\omega$ corresponds to the bandwidth of the shear wave excitation, FT is the Fourier transform, and d is the displacement of the medium as a function of the spatial coordinates and the time, t.

C. Mechanical testing for the shear elasticity of phantom materials

For each phantom material, 6 cylindrical specimens with a diameter of 26 mm and a height of ~17.5 mm were assessed using an Instron 3345 (Norwood, MA, US) where the samples were compressed at 2 mm/s, which corresponds to a strain rate of 12%/s. Since the phantom materials are approximately incompressible, the Poisson's ratio, ν, is ~0.5, and therefore the shear modulus is ~1/3 of the Young's modulus (E).

D. Tissue-mimicking phantoms

Gelatin (Sigma Co., St. Louis, USA) and agar (Alfa Aesar, MA, USA) were used in this study to fabricate tissue-mimicking phantoms. These phantoms possess shear moduli ranging from 1 to ~30 kPa. Normal breast tissues typically have a shear modulus of 1-13 kPa and the shear modulus of malignant lesions is ~50 kPa [7]. Two percent w/v fiber powder was added in the phantoms as scattering media for US imaging. Three dimensional mapping of the shear modulus of an *ex vivo* syngeneic mouse tumor was then obtained by embedding a roughly spherical neu deletion line (NDL) tumor within an 8% gelatin phantom. All studies were performed using available *ex vivo* tissue and were approved by the relevant UC Davis institutional authorities.

E. 3D reconstruction of tumor inclusion

To fully characterize a tumor inclusion embedded in a phantom, the MR-guided transient shear wave imaging was performed in equally-spaced parallel planes. A threshold value of 16 kPa, which is larger than the shear modulus of the background (phantom) material, was applied to segment the background and tumor regions. By combining the elasticity maps from various slices, a 3D reconstruction of the embedded tumor was obtained.

III. RESULTS

A. Visualization of transient shear wave propagation

Using the t-MRE technique, the propagating shear wave was readily visualized in a 1.5% w/v gelatin and 1.5% w/v agar phantom (Fig. 2a) with planar shear wave travel distances of 3 to 26 mm. The total acquisition time for each displacement map was 4 min, which resulted in a total of 36 min for all maps at 9 time delays.

Shear wave propagation was also observed in the same phantom using USgSWI method. Fifty frames were acquired after each 3-push excitation and the resulting images were averaged over 20 acquisitions. A set of nine images from time points 0.4 to 3.6 ms was selected (Fig. 2b) to compare with MR results at similar time points.

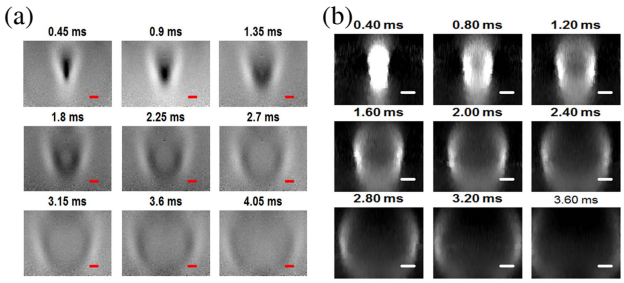

Fig. 2. Visualization of shear wave propagation under both MR and US guidance. (a) Typical example of t-MRE in phantom 1. A series of 9 consecutive images demonstrated the wave propagation by varying the delay time t_d from 0.45 ms to 4.05 ms by steps of 0.45 ms. (b) Shear wave propagation in phantom 1 using US shear wave imaging. Nine images at similar time points were chosen to compare with the t-MRE results. The scale bars represent 5 mm.

Shear modulus maps were created based on the MRI and US techniques and shear modulus estimates were overlaid in the colored parametric images based on MR (Fig. 3a) and US (Fig. 3b) methods. The shear modulus was estimated as 27.3

± 2.3 kPa with MR using the TOF method based on Eq. 1 (n=3). Similarly, the shear modulus estimate was 28.2 ± 2.3 kPa with US using the LIM as described in Eq. 2 (n=3). The MT estimate of the shear modulus was 32.3 ± 1.8 kPa (n=6). No significant difference was observed between these techniques (Fig. 3c).

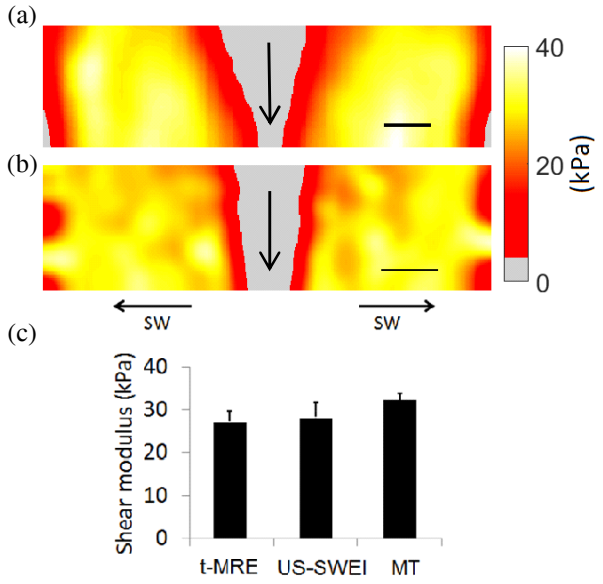

Fig. 3. Comparison of the shear modulus measured by MR, US and mechanical testing (MT). (a) MR elasticity map calculated using the time-of-flight (TOF) method. US excitation occurred at the location of the arrow and therefore the shear modulus is not estimated in this region. (b) US elasticity map calculated using the local inversion method (LIM) and based on US excitation at the location of the arrow. (c) The estimated shear moduli (mean ± standard deviation) were 28.2 ± 2.3 (n=3), 27.3 ± 2.3 (n=3) and 32.3 ± 1.8 kPa (n=6) from US, MR and mechanical testing, respectively.

B. Shear elasticity assessment of gelatin phantom with an agar inclusion

In order to demonstrate the feasibility of lesion detection, the t-MRE protocol was tested on an 8% w/v gelatin phantom with a 1% w/v agar "lesion" inclusion (Fig. 4a). The expected change in the speed of sound was observed after the wave encountered the inclusion and reflection from the gelatin-agar interface was also observable. A parametric image of shear modulus estimated from the shear wave images using the TOF method is shown in Fig. 4b, where the agar inclusion can be clearly distinguished from the gelatin background. The estimated shear modulus was 13.8 ± 2.2 kPa (n =3) in the agar inclusion and 7.5 ± 0.3 kPa (n=3) in the gelatin with results from three replicates summarized in Fig. 4c.

For comparison, the same gelatin phantom was imaged with the USgSWI method (Fig. 5a). The wave evolution was visualized and and a parametric image of the estimated shear modulus using the LIM is shown in Fig. 5b. The shear modulus was estimated as 12.8 ± 1.0 kPa in the agar inclusion (n=3) and 7.9 ± 0.8 kPa in the gelatin (n=3) (Fig. 5c). Estimates of the shear modulus of the background gelatin were consistent between slices; however, a range of 11.9-13.5 kPa was observed between successive estimates of the shear modulus in the inclusion obtained by rotating the sample between data acquisitions.

C. 3D reconstruction

Five images were acquired spanning the tumor diameter, with 1 mm spacing between acquisitions and the corresponding shear elasticity maps were then generated (Fig. 6a). The estimated shear modulus was 4.3 ± 0.4 kPa in 8% gelatin and 19.2 ± 5.1 kPa in the NDL tumor and the elasticity of the background medium and tumor inclusion was consistent across multiple planes (Fig. 6b). With a threshold of 16 kPa, the tumor was clearly distinguished from the surrounding medium based on the elasticity maps (Fig. 6c).

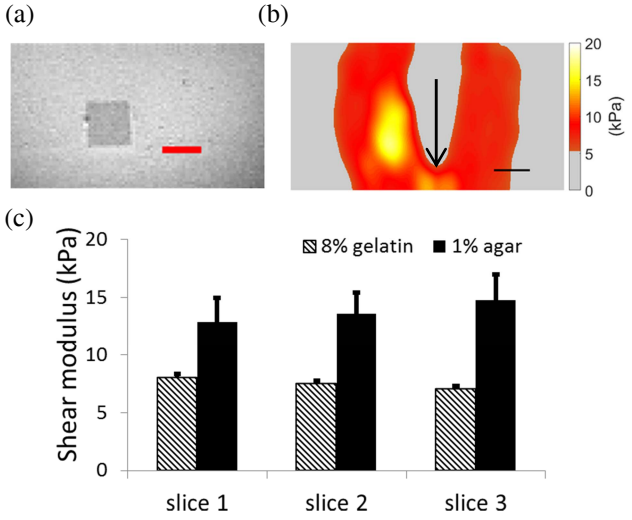

Fig. 4. Shear modulus estimation in an 8% gelatin phantom with 1% agar inclusion using t-MRE. (a) MR magnitude image. (b) Parametric image of the shear modulus using the TOF method. US excitation occurred at the location of the arrow. (c) Comparison of the estimated shear moduli in both gelatin and agar from three successive slices within the inclusion.

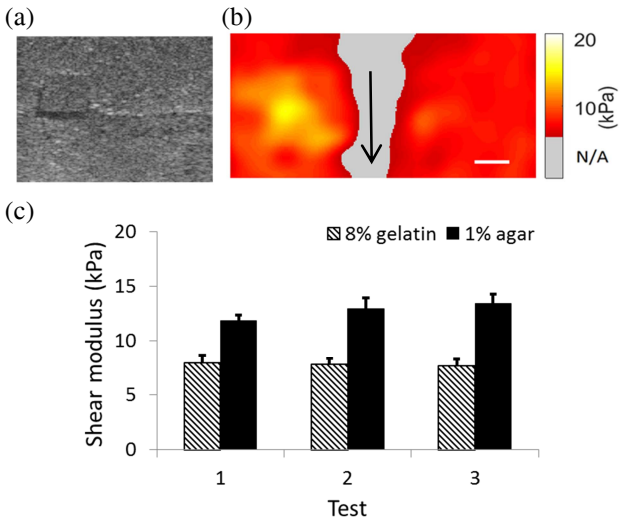

Fig. 5. The shear modulus estimates in an 8% gelatin phantom with 1% agar inclusion using USgSWI. (a) B-mode image. (b) Parametric image of shear modulus using the LIM including the location of the US stimulus (arrow). (c) Comparison of the estimated shear moduli in both gelatin and agar rotated by approximately 90 degrees between repetitions.

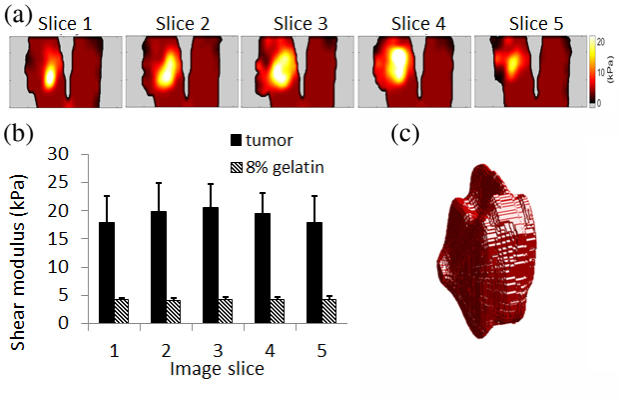

Fig. 6. 3D reconstruction of NDL tumor inclusion. (a) Five MR elasticity maps reconstructed from successive slices separated by 1 mm. (b) Summary of the shear moduli in gelatin and the tumor inclusion. (c) The reconstructed 3D image based on the elasticity maps from A.

IV. Discussion and Conclusion

We demonstrated for the first time that supersonic techniques can be incorporated into MRI-based shear wave imaging and quantitative elastography. The resulting quasi-planar wavefront is easily visualized by MRI and the displacement and wave velocity are readily quantified. For phantoms with a range of shear modulus between 8 and 32 kPa, we demonstrated that both US and MR-based shear wave imaging techniques can be applied to visualize changes in the propagating shear wave that result from differences in the properties of the media. Using the new t-MRE sequence, we observed shear waves travelling over distances between 2 and 30 mm. Differences in shear modulus estimates between t-MRE and USgSWI methods and MT were less than 7% of the MT value.

The t-MRE protocol has potential application in monitoring tissue stiffness during HIFU treatments. Ongoing work is aimed at the detection of ablation foci.

Acknowledgements

The work has been supported by NIHR01CA134659, NIHR01CA210553 and NIH R01CA199658.

References

[1] M. A. Aguilo, W. Aquino, J. C. Brigham, and M. Fatemi, "An inverse problem approach for elasticity imaging through vibroacoustics," *IEEE Trans Med Imaging,* vol. 29, pp. 1012-21, Apr 2010.

[2] J. Bamber, D. Cosgrove, C. F. Dietrich, J. Fromageau, J. Bojunga, F. Calliada, V. Cantisani, J. M. Correas, M. D'Onofrio, E. E. Drakonaki, M. Fink, M. Friedrich-Rust, O. H. Gilja, R. F. Havre, C. Jenssen, A. S. Klauser, R. Ohlinger, A. Saftoiu, F. Schaefer, I. Sporea, and F. Piscaglia, "EFSUMB guidelines and recommendations on the clinical use of ultrasound elastography. Part 1: Basic principles and technology," *Ultraschall Med,* vol. 34, pp. 169-84, Apr 2013.

[3] D. Cosgrove, F. Piscaglia, J. Bamber, J. Bojunga, J. M. Correas, O. H. Gilja, A. S. Klauser, I. Sporea, F. Calliada, V. Cantisani, M. D'Onofrio, E. E. Drakonaki, M. Fink, M. Friedrich-Rust, J. Fromageau, R. F. Havre, C. Jenssen, R. Ohlinger, A. Saftoiu, F. Schaefer, and C. F. Dietrich, "EFSUMB guidelines and recommendations on the clinical use of ultrasound elastography. Part 2: Clinical applications," *Ultraschall Med,* vol. 34, pp. 238-53, Jun 2013.

[4] E. Bavu, J. L. Gennisson, M. Couade, J. Bercoff, V. Mallet, M. Fink, A. Badel, A. Vallet-Pichard, B. Nalpas, M. Tanter, and S. Pol, "Noninvasive in vivo liver fibrosis evaluation using supersonic shear imaging: a clinical study on 113 hepatitis C virus patients," *Ultrasound Med Biol,* vol. 37, pp. 1361-73, Sep 2011.

[5] S. Chen, W. Sanchez, M. R. Callstrom, B. Gorman, J. T. Lewis, S. O. Sanderson, J. F. Greenleaf, H. Xie, Y. Shi, M. Pashley, V. Shamdasani, M. Lachman, and S. Metz, "Assessment of liver viscoelasticity by using shear waves induced by ultrasound radiation force," *Radiology,* vol. 266, pp. 964-70, Mar 2013.

[6] J. Bercoff, M. Tanter, and M. Fink, "Supersonic shear imaging: a new technique for soft tissue elasticity mapping," *IEEE Trans Ultrason Ferroelectr Freq Control,* vol. 51, pp. 396-409, Apr 2004.

[7] M. Tanter, J. Bercoff, A. Athanasiou, T. Deffieux, J. L. Gennisson, G. Montaldo, M. Muller, A. Tardivon, and M. Fink, "Quantitative assessment of breast lesion viscoelasticity: initial clinical results using supersonic shear imaging," *Ultrasound Med Biol,* vol. 34, pp. 1373-86, Sep 2008.

[8] M. W. Urban, S. Chen, and M. Fatemi, "A Review of Shearwave Dispersion Ultrasound Vibrometry (SDUV) and its Applications," *Current medical imaging reviews,* vol. 8, pp. 27-36, 2012.

[9] A. P. Sarvazyan, O. V. Rudenko, S. D. Swanson, J. B. Fowlkes, and S. Y. Emelianov, "Shear wave elasticity imaging: a new ultrasonic technology of medical diagnostics," *Ultrasound Med Biol,* vol. 24, pp. 1419-35, Nov 1998.

[10] R. Muthupillai, D. J. Lomas, P. J. Rossman, J. F. Greenleaf, A. Manduca, and R. L. Ehman, "Magnetic resonance elastography by direct visualization of propagating acoustic strain waves," *Science,* vol. 269, pp. 1854-7, Sep 29 1995.

[11] R. Muthupillai, P. J. Rossman, D. J. Lomas, J. F. Greenleaf, S. J. Riederer, and R. L. Ehman, "Magnetic resonance imaging of transverse acoustic strain waves," *Magn Reson Med,* vol. 36, pp. 266-74, Aug 1996.

[12] K. Nightingale, M. S. Soo, R. Nightingale, and G. Trahey, "Acoustic radiation force impulse imaging: In vivo demonstration of clinical feasibility," *Ultrasound in Medicine and Biology,* vol. 28, pp. 227-235, Feb 2002.

[13] F. L. Lizzi, R. Muratore, C. X. Deng, J. A. Ketterling, S. K. Alam, S. Mikaelian, and A. Kalisz, "Radiation-force technique to monitor lesions during ultrasonic therapy," *Ultrasound Med Biol,* vol. 29, pp. 1593-605, Nov 2003.

[14] Y. Liu, B. Z. Fite, L. M. Mahakian, S. M. Johnson, B. Larrat, E. Dumont, and K. W. Ferrara, "Concurrent Visualization of Acoustic Radiation Force Displacement and Shear Wave Propagation with 7T MRI," *PLoS One,* vol. 10, p. e0139667, 2015.